High Temperatures - High Pressures, 1975, volume 7, pages 481-496

Sound velocity and equation of state of liquid mercury and bismuth at simultaneous high pressure and temperature

H A Spetzler¶, M D Meyer#
Sandia Laboratories, Livermore, California 94550, USA
Tin Chan
Cooperative Institute for Research in Environmental Sciences, University of Colorado, Boulder, Colorado 80302, USA
Received 2 February 1975, in revised form 1 September 1975

Abstract. Equation of state parameters are uniquely defined when sound velocity measurements in pressure-temperature domain are combined with heat capacity and thermal expansion measurements as functions of temperature at zero pressure. An experimental approach to obtaining such measurements for molten metals is described. Data for liquid mercury and bismuth are presented to temperatures of 1000 K and pressures up to 1 GPa (10 kbar), corresponding to volume changes up to 18%. Although both bismuth and mercury are anomalous metals, experimental results as well as theoretical considerations suggest a tendency toward normal liquid metal behavior at large volumes.

List of symbols

C_P	specific heat at constant pressure	P	pressure
C_V	specific heat at constant volume	T	temperature
E	energy	T_m	melting temperature at room pressure
E_F	Fermi energy		
f	repetition frequency	v	sound velocity
F	normalized frequency	v_0	normalization velocity
g	$n(E_F)/n_f(E_F)$, pseudogap parameter	V	volume
		V_m	value of V at melting point
g_m	value of g at melting	V_0	normalization volume
k	Boltzmann's constant	Z	valency
K_S	adiabatic bulk modulus	α	thermal expansion coefficient
K_T	isothermal bulk modulus	γ	Grüneisen parameter
l	sample length	ϵ	small pressure increment
L	normalized sample length	η	packing fraction
M	atomic mass	η_V	packing fraction at constant volume
$n(E)$	electron density of states at energy E	ρ	density
$n_f(E)$	free electron density of states at E	τ	time of flight
N	order of interference	ϕ	r.f. frequency
N_i	ionic density	Ω	atomic volume

1 Introduction

A method for determining the equation-of-state parameters of a material consists of measuring the ultrasonic velocities in a temperature-pressure domain. These velocities, along with thermal expansion and specific heat data over the same temperature range at zero pressure, are sufficient for determining the thermodynamic variables of the material within this P-V-T domain (Davis and Gordon, 1967; Spetzler *et al.*, 1972). A method first developed by McSkimin (1961) involves measuring sound velocities by ultrasonic interferometry. Here we report the first data for molten metals over a substantial range of simultaneous high pressure and temperature obtained by a modified and automated version of McSkimin's method.

¶ Now at Cooperative Institute for Research in Environmental Sciences, University of Colorado, Boulder, Colorado 80302, USA.
# Now at Lawrence Livermore Laboratories, Livermore, California 94550, USA.

Sound velocity measurements were made for bismuth and mercury in their liquid state from just above their melting temperature to ~1000 K and from atmospheric pressure up to 1 GPa (10 kbar). The volume changes for bismuth and mercury in our experimental range were 9% and 18% respectively. The data are reduced to yield equation-of-state parameters and are then compared with those obtained by various theoretical model calculations.

2 Experimental arrangement

2.1 *Sample holder*

The ultrasonic measurements were made in a high-pressure chamber with an internal furnace. The sample vessel is shown in figure 1. It consists of three main parts: (i) the buffer rod; (ii) the sample housing; and (iii) an aluminum oxide reflector with a sample expansion chamber. A quartz transducer is mounted on the bottom of the buffer rod. The sample is contained between the reflector and the buffer rod by a tungsten spacer. The bottom surface of the reflector, the flat surfaces of the tungsten spacer and the mating surface of the quartz buffer rod are lapped to a tenth of the wavelength of sodium light. This provides a seal to contain the molten metal. Two thermocouples are provided to measure the temperature: one goes down midway between the aluminum oxide reflector and the quartz buffer rod with the end of the thermocouple in the middle of the tungsten spacer; the other goes to the bottom of the aluminum oxide reflector thus to the top of the sample. The reflector has an expansion chamber which allows for sample overflow. The three parts are held together with a tungsten sleeve. The pressure necessary to seal the assembly is provided by a tungsten spring at the buffer rod end. The vent hole in the expansion chamber allows the pressure medium (in this case argon) to enter and pressurize the system. The pressure is generated by a conventional 1·5 GPa (15 kbar) pressure system.

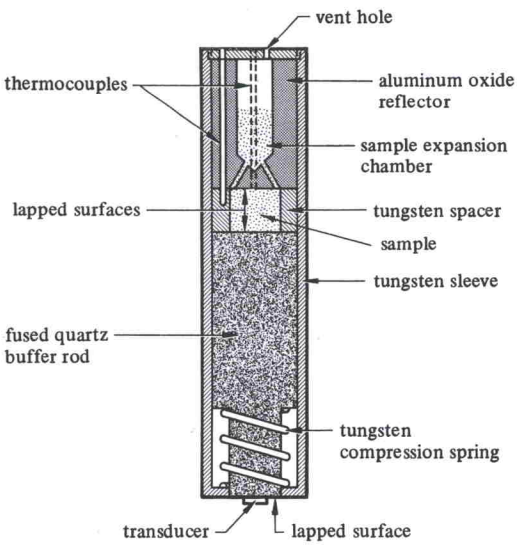


Figure 1. Sample holder for sound velocity measurements in molten metals. The sound velocity is measured by observing the time delay between acoustic signals reflected from the lapped surfaces (spacing ~8 mm) above and below the sample.

2.2 *Sample preparation*

To load the sample, the sample vessel is placed in a small furnace within a glove box. The atmosphere in the glove box is mainly argon, which contains ~20% carbon monoxide. The carbon monoxide serves as a getter to produce a reducing atmosphere

and thus prevent oxidation of the sample. In the case of bismuth, the sample vessel without the reflector is placed in the furnace and heated above the melting temperature of bismuth. At this point bismuth is introduced into the sample space. Wetting between buffer rod and sample often presents difficulties. To assure good wetting, the transducer is excited such that echoes appear on the oscilloscope from the end of the buffer rod. When wetting is achieved, the magnitude of the reflection between the buffer rod and the sample is greatly decreased. When the free surface of the sample is parallel to the end of the buffer rod, an echo from the free end of the sample is observed. Initial wetting is achieved at a temperature of ~100–200 K above the melting temperature of bismuth. Scraping the surface of the buffer rod with ceramic or tungsten tools enhances wetting. Once wetting has been achieved, the aluminum oxide reflector is wrung onto the top of the tungsten spacer. Additional bismuth is added until the expansion chamber is approximately half filled. At this point a good signal from the buffer rod–sample as well as the sample–reflector interface should be visible on the oscilloscope. If the temperature is now lowered, the signal remains until the sample freezes, at which point it vanishes. Upon reheating the sample, the signal reappears in the vicinity of the melting point or slightly above. After several heating and cooling cycles the sample vessel is allowed to cool to room temperature. At this time the sample vessel is inserted into the furnace assembly which goes into the high-pressure vessel. A plastic bag containing the atmosphere in the glove box is placed around the sample and furnace while it is transported to the high pressure vessel. This vessel is flushed with argon before the sample is carefully inserted.

2.3 *Sample furnace*

The furnace (see figure 2) consists of three segments. Each of the segments consists of two windings which are bifilar; that is they are wound in opposite directions on two different levels to minimize magnetic fields. The three segments are necessary to prevent convection and to achieve a low temperature gradient over the sample space. By being able to control the power to each of the segments separately, it is possible to eliminate convection within the vicinity of the sample. The power is supplied

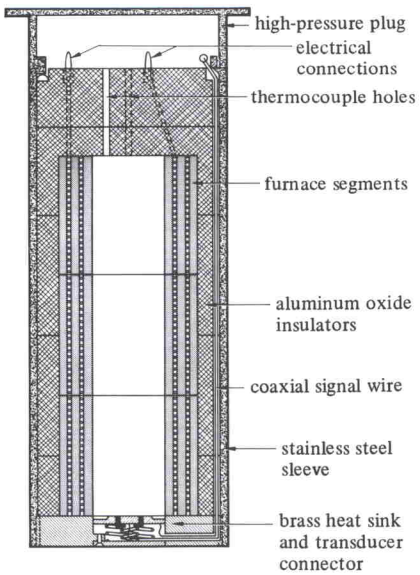


Figure 2. Sample furnace with three bifilar wound segments. Space for sample holder is 19 mm in diameter by 150 mm long.

from a proportional controller which is controlled from the thermocouple at the center of the sample. The power supplied from the proportional controller is then distributed by three separate powerstats to the three windings. The setting of the powerstats is determined such that the temperature difference between the top and the center thermocouple is at a minimum. The temperature difference can usually be adjusted to be less than 5 K. The wire used in the furnace is 0·75 mm diameter tungsten or molybdenum. Immediately surrounding the furnace segments are aluminum oxide spacers which serve as insulators to avoid great heat loss between the furnace segment and the walls of the pressure vessel. The furnace is designed such that the joints between the insulators do not overlap with the joints between the furnace segments, thus further reducing the possibility for convection. Tight tolerances are observed to minimize the gas volume and convection problems. The transducer connector is mounted on the bottom of the furnace and is constructed of brass to keep the transducer and the bottom end of the buffer rod at relatively low temperatures (<473 K). The sample vessel is constructed so that the sample is in the middle of the central furnace segment. A stainless steel sleeve and a flat spring hold the furnace assembly together. The coaxial signal wire runs from the transducer on the outside of the furnace to the top, where it and the other electrical connections mate with the high-pressure plug containing all the high-pressure electrical feedthroughs.

3 Determination of the equation of state

3.1 *Sound velocity measurement*

The ultrasonic velocity measurements were taken by an automated version (Spetzler, 1970) of the phase comparison technique originally proposed by McSkimin (1961). A detailed description of the automated version is in preparation, and a block diagram and envelopes of echo patterns are shown in figure 3.

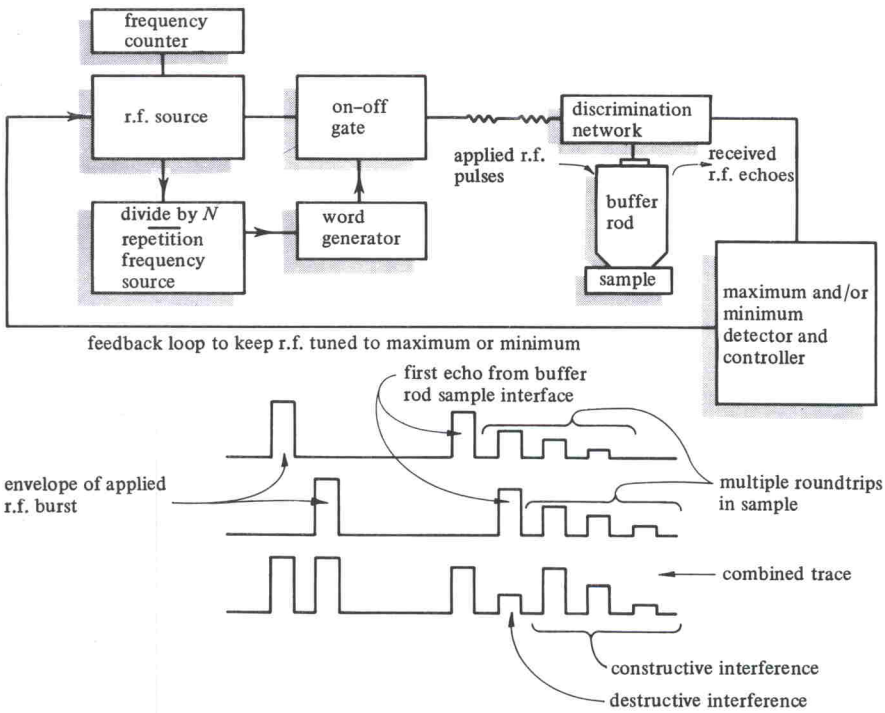


Figure 3. Block diagram of the velocity measuring system incorporating automatic tracking and pulse-spacing adjustments.

In short, an r.f. source (frequency range 10 to 60 MHz) is gated such that echoes of two consecutive bursts overlap. If the time for one round trip of the ultrasonic signal through the sample corresponds to an integer or half integer multiple of the period of the r.f. signal, constructive or destructive interference occurs between the echoes. To obtain the first precise overlap of the echoes this spacing must correspond to one round trip time in the sample, i.e. the repetition frequency which controls the r.f. burst spacing must be a submultiple of the signal frequency. Once the number of wavelengths, N, in the sample has been determined, it is an easy matter to lock the repetition frequency to the r.f. by simply dividing the latter by N. A maximum and/or minimum detector and controller employing a lock-in amplifier senses a maximum or minimum interference condition and adjusts the signal frequency to maintain that condition. As the temperature and pressure environment of the sample is changed, the length of the sample and sound velocity in it, and therefore the signal frequency where interference occurs changes as well. When the system is locked onto a particular interference condition, the r.f. will follow any changes in environment, i.e. it will maintain the same value of N and adjust the burst repetition frequency automatically.

The sound velocity v in the sample can be expressed in terms of the length of the sample l, the signal frequency ϕ, the repetition frequency f, and its inverse, the period τ, by

$$v = \frac{2l}{\tau} = 2lf = \frac{2l\phi}{N} \ . \tag{1}$$

To determine the sound velocity as a function of temperature and pressure, both the length and the appropriate signal frequency must be determined. In our case the length of the sample is controlled by the tungsten spacer and therefore by the equation of state of tungsten (Featherston and Neighbours, 1963; Ivanov, 1969). It is perhaps simplest to express the velocity in terms of a reference velocity and normalized length L and frequency F such that

$$v = v_0 LF \ . \tag{2}$$

In our case v_0 and the normalization for mercury are measured under room conditions ($T \sim 300$ K, $P = 1$ atm), and for bismuth also at atmospheric pressure but at its melting temperature. These are referred to as initial conditions throughout the paper.

3.2 *Data reduction*

A complete equation of state for the liquid is determined when the frequency data measured over a range in temperature and pressure are combined with specific heat and thermal expansion data measured as functions of temperature at zero pressure. Specific heat measurements on molten metals have successfully been made to several thousand degrees and the results are reported by Margrave (1970). The problem of containing the corrosive molten metal is overcome by levitating and simultaneously heating the sample with r.f. energy, as in an induction heater. Upon reaching the appropriate temperature, the sample is dropped into a calorimeter. We have successfully demonstrated that the thermal expansion coefficient can be measured by holographic interferometry while a molten ball of metal is levitated (Spetzler *et al.*, 1974).

In reducing the ultrasonic data we proceed in a fashion similar to that used by Davis and Gordon (1967) and Spetzler *et al.* (1972). Here we shall only present a short outline. The data are taken along isotherms for increasing and decreasing pressure. Temperature, pressure, and frequency are recorded. If the initial velocity, the equation of state of tungsten (i.e. the length of the chamber), and N are known, the frequency

data can readily be converted to velocity data by equation (2). The normalized length can then be assumed to be available from a subprogram in a computer. An equation of state of a material is determined if, for example, the relation between volume, temperature, and pressure are known. In the case of these ultrasonic data, only the travel time through a sample is directly determined; the volume may be calculated from the compressibility and thermal expansion of the material.

The adiabatic bulk modulus K_S is related to the sound velocity and the density by the relation

$$K_S = \rho v^2 \,. \tag{3}$$

Although the sound velocity is adiabatic, the sample is subjected to isothermal conditions. To calculate the density of the sample we therefore need the isothermal bulk modulus

$$K_T = \rho\left(\frac{\partial P}{\partial \rho}\right)_T = \frac{K_S}{1+\alpha\gamma T} \,, \tag{4}$$

where

$$\gamma = \frac{\alpha K_S}{\rho C_P} = \frac{\alpha v^2}{C_P} \tag{5}$$

is the Grüneisen parameter. With the thermal expansion coefficient α and C_p known as functions of temperature at zero pressure, we also know ρ, and can calculate the isothermal bulk modulus and therefore a new density at $P = 0+\epsilon$ as a function of temperature. ϵ is a small integration step. To integrate further into the pressure domain it is necessary to find α and C_P as functions of temperature at $P = 0+\epsilon$, i.e. we must use the pressure derivative of α and C_P. From thermodynamic identities we find

$$\left(\frac{\partial \alpha}{\partial P}\right)_T = \frac{1}{K_T^2}\left(\frac{\partial K_T}{\partial T}\right)_P \tag{6}$$

and

$$\left(\frac{\partial C_P}{\partial P}\right)_T = -\frac{T}{\rho}\left[\left(\frac{\partial \alpha}{\partial T}\right)_P + \alpha^2\right] \,. \tag{7}$$

It is possible to continue this integration and calculate the equation of state parameters throughout the pressure and temperature domain where frequency data exist. A computer program has been written which simultaneously integrates the above equations and calculates the equation of state parameters.

4 Results and comparison with theory

4.1 *Results*

The experimental results for the velocity of sound and the deduced density for mercury and bismuth are shown in figures 4 and 5 as functions of temperature and pressure. Figure 6 illustrates the Grüneisen parameters for these two metals. Selected values of other equation of state parameters are given in table 1. Data for mercury at temperatures above 629·58 K under ambient pressure refer to a hypothetical state of the system unrealizable in practice. These values were obtained by polynomial extrapolation of the experimental results obtained at higher pressure where these temperatures could be reached.

Some salient features in the thermodynamic properties of the two liquid metals can be noted here. For example $(\partial v/\partial T)_P$ and $\partial(\partial v/\partial P)_T/\partial T$ for mercury are several times larger than those for bismuth. However, the increase of $(\partial v/\partial T)_P$ as a function

of temperature is much more pronounced for bismuth. It is interesting to observe that if the reduced temperature T/T_m (where T_m is the melting temperature at room pressure) is used in place of T, then the difference in the magnitudes of $(\partial v/\partial T)_P$ and $\partial(\partial v/\partial P)_T/\partial T$ becomes greatly reduced. The values of the Grüneisen parameter γ for both liquid mercury and liquid bismuth fall into the same general range as for solid metals. In contrast to the solids, however, γ decreases with volume along isotherms in both liquids. For both molten metals the isothermal volume derivative $(\partial\gamma/\partial V)_T$ decreases with increasing temperature. At constant volume, however, γ increases as a function of temperature for bismuth just above its melting point. This isochoric temperature dependence decreases with rise of temperature so that γ becomes virtually independent of T at about 800 K. In contrast to bismuth, for mercury γ at constant volume decreases with T. As in bismuth, this temperature dependence also becomes less strong at high temperatures. Temperature independence seems to be approached just above our experimental range at ~1200 K.

It is perhaps impossible to calculate an absolute accuracy for the thermodynamic data presented here. The reproducibility of the frequency (and therefore velocity) measurements at a given temperature and pressure is to within a few parts in 10^5. In the case of a cubic solid where several sound velocities can be measures in several crystalline directions it is possible to perform a redundancy check and get a better understanding of the accuracy of the measurements. This was done by Spetzler *et al.* (1972) for NaCl. On the basis of that work we estimate that the pressure and temperature derivatives given in table 1 are in error at most by one to two percent.

Table 1. Selected equation-of-state parameters for mercury and bismuth.

P (GPa)	T	v	$\left(\frac{\partial v}{\partial T}\right)_P$	$\left(\frac{\partial v}{\partial P}\right)_T$	K_S	$\left(\frac{\partial K_S}{\partial T}\right)_P$	$\left(\frac{\partial K_S}{\partial P}\right)_T$	γ	α_S
Mercury									
0	300	1·450	−42·4	2·117	2·845	−2·18	9·68	2·74	1·813
	550	1·334	−50·6	2·79	2·299	−2·17	11·74	2·43	1·846
	750	1·227	−56·0	3·38	1·873	−2·09	13·57	2·23	2·031
	950	1·110	−60·4	4·04	1·468	−1·95	15·51	2·07	2·404
0·4	300	1·532	−35·1	1·91	3·222	−2·01	8·76	2·80	1·660
	550	1·436	−41·2	2·33	2·719	−2·00	10·16	2·49	1·619
	750	1·349	−45·1	2·76	2·323	−1·94	11·53	2·30	1·688
	950	1·256	47·9	3·27	1·943	−1·84	13·09	2·14	1·851
0·8	300	1·604	−30·9	1·72	3·582	−1·93	8·08	2·85	1·543
	550	1·521	−35·1	1·95	3·103	−1·89	8·77	2·53	1·465
	750	1·449	−37·3	2·21	2·732	−1·81	9·63	2·34	1·480
	950	1·373	−38·6	2·56	2·378	−1·71	10·73	2·20	1·556
Bismuth									
0	550	1·648	−8·97	2·13	2·729	−0·632	8·22	2·19	1·227
	750	1·623	−15·83	2·20	2·582	−0·829	8·32	2·18	1·259
	950	1·584	−22·69	2·37	2·399	−0·997	8·76	2·13	1·291
0·4	550	1·729	−7·96	1·90	3·051	−0·633	7·55	2·27	1·153
	750	1·707	−13·62	2·00	2·907	−0·803	7·77	2·24	1·167
	950	1·674	−19·29	2·11	2·731	−0·951	8·02	2·18	1·178
0·8	550	1·800	−5·49	1·68	3·357	−0·572	6·86	2·34	1·094
	750	1·783	−11·79	1·80	3·221	−0·779	7·19	2·31	1·095
	950	1·753	−18·10	1·84	3·047	−0·962	7·25	2·23	1·092

Units used in this table are as follows: P in GPa, T in K, v in 10^3 m s^{-1}, $(\partial v/\partial T)_P$ in 10^{-2} m s^{-1} K^{-1}, $(\partial v/\partial P)_T$ in 10^{-7} m s^{-1} Pa^{-1}, K_S in 10^{10} Pa, $(\partial K_S/\partial T)_P$ in 10^7 Pa K^{-1}, $(\partial K_S/\partial P)_T$ in 10^3 (dimensionless), α in 10^{-4} K^{-1}, and γ is dimensionless.

The possibility of the pressure medium dissolving in the molten metal and affecting the measurements was checked. Argon, because of its large atomic size, was used as the pressure medium. Spot checks of the data were made with helium as the pressure medium, and no differences in the data were discernible.

4.2 *Comparison with previous experimental work*

Sonic velocity in liquid mercury has previously been measured by Seemann and Klein (1965) in the temperature range 238 to 321·3 K under a small pressure, and by Davis and Gordon (1967) at 294·9, 313·5 and 325·9 K in the pressure range 10^5–$1{\cdot}3 \times 10^9$ Pa. Some of their results are plotted in figure 4a for comparison. For the sake of clarity only values at 313·5 K at pressures of 10^5, 2×10^8, 4×10^8, 6×10^8, 8×10^8, and $1{\cdot}0 \times 10^9$ Pa of the velocity data given by Davis and Gordon (1967) are included. It is clearly seen that where the temperature and pressure domains overlap our results are in excellent agreement with those of the two previous groups.

Similar comparison for the sound velocity in liquid bismuth is made in figure 4b. The previous data plotted are taken from Jarzynski (1963), Gitis and Mikhailov (1965), and Flinn *et al.* (1971). All the previous workers have made their measurements under small pressures which can be considered zero for our purpose. Our results agree almost exactly with those of Flinn *et al.*, but have values about 3% lower than those given by Gitis and Mikhailov. The slope of our 'zero pressure' isobar, on the other hand, is very similar to that of the Russian authors. Both our

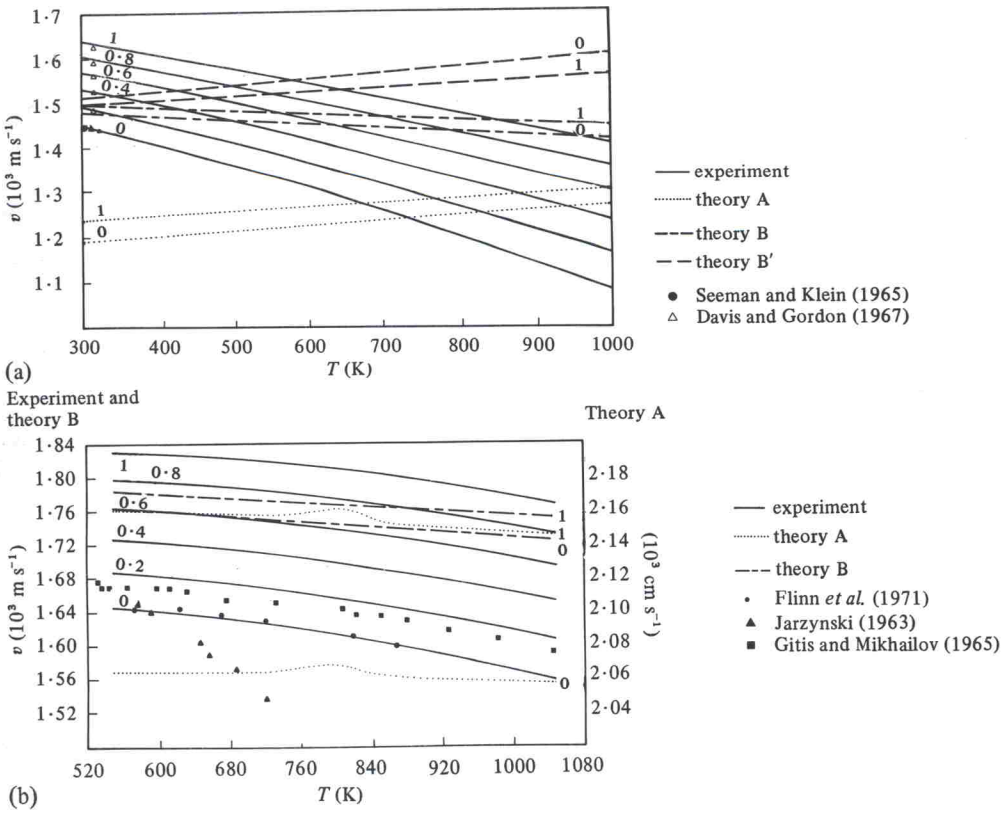


Figure 4. Velocity of sound for (a) liquid mercury and (b) liquid bismuth plotted as a function of temperature for different pressures (shown in GPa against the curves) and compared with theory. See text for description of various theories. Results of previous experiments are plotted for comparison. Only those data points falling within our T–P range have been included.

isobar and theirs show a change in slope around 800–850 K. The results obtained by Jarzynski differ drastically in both magnitude and slope from ours as well as from any others. Jarzynski (Flinn *et al.*, 1971) has indicated that his velocities may be in error.

In figure 5a our derived density data for mercury are compared with the results of previous workers. Sources of data and other relevant information are listed in table 2. Only those data falling within our temperature–pressure domain have been plotted. Our results are in very close agreement with those of Davis and Gordon (1967) and Grindley and Lind (1971). The data of Postill *et al.* (1968) at 0·1 GPa (1 kbar) fall approximately in the middle of our 0 and 0·2 GPa (2 kbar) curves below 700 K, but show a flatter slope at higher temperatures. Similarly, the 0·2 GPa (2 kbar) and 0·4 GPa (4 kbar) isobars given by Kikoin and Senchankov (1967) coincide with ours below 775 and 575 K, respectively, but in contrast to the results of Postill *et al.*, slopes of their isobars become steeper than ours at higher temperatures. The data points of Even and Jortner (1974) are at variance with other investigations, including the present work. We do not understand the reason for this discrepancy. We should perhaps also point out that a large portion of the measurements in the references cited above were made in the vapor state and are therefore not suitable for comparison with the present work. No previous results for the density of liquid bismuth are available for comparison.

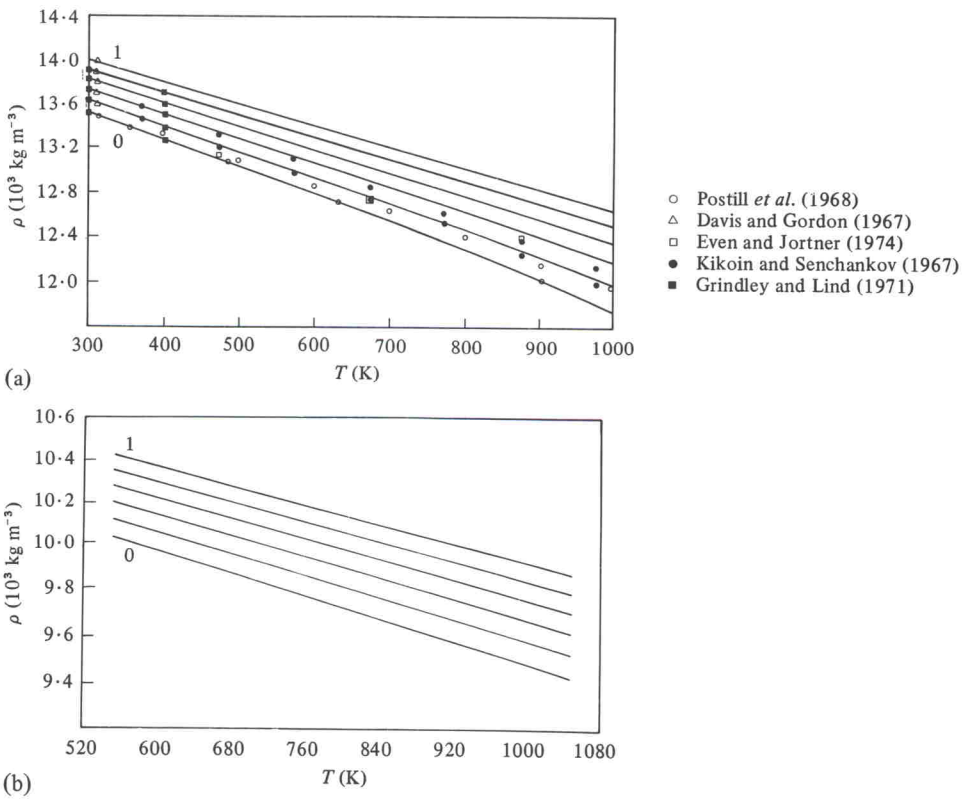


Figure 5. Density for (a) liquid mercury and (b) liquid bismuth, derived from the results shown in figure 4, plotted as a function of temperature for different pressures (shown in GPa against the curves). Earlier results for mercury are included for comparison. Only those data points falling within our T–P range are included.

Table 2. Some experimental work on density of mercury.

Reference	Method	Temperature and pressure domain	Data used in figure 5
Davis and Gordon (1967)	sonic velocity and thermodynamically derived density	294·9 K, 313·5 K, 325·9 K; to 1·3 GPa	313·5 K; 0·2, 0·4, 0·6, 0·8, 1 GPa
Kikoin and Senchankov (1967)	γ radiation from ^{203}Hg	273–2273 K; to 0·5 GPa	373–973 K; 0·2, 0·4 GPa
Postill *et al.* (1968)	Archimedes' method	293–1373 K; to 0·1 GPa	316–942·5 K; $P = 0$; 400–1000 K, 0·1 GPa
Grindley and Lind (1971)	displacement transducer (LVDT)	303–423 K; to 0·8 GPa	303 K, 403 K; 0–0·8 GPa
Even and Jortner (1974)	capacitive expansion method	293–1723 K; to 0·15 GPa	473 K, 673 K, 873 K; 0·1 GPa
Bridgman (1949)	piezometer	273 K, 293 K; to 1·2 GPa	temperatures below our range
Present work	sonic velocity and thermodynamically derived density	300–1000 K; to 1 GPa	300–1000 K; to to 1 GPa

4.3 *Comparison with theory*

We attempted to gain further insight into the nature of molten bismuth and mercury, and possibly of molten metals in general, by comparing our measurements with theory. It should be pointed out that no really satisfactory theory for the velocity of sound in liquid metals (comparable in rigor to those for electrical resistivity and electronic structure) is available at present. We shall employ two different existing theories. One theory is that due to Ascarelli (1968) (hereafter referred to as theory A) which uses a simple model of hard spheres immersed in a uniform background potential. The other is Bohm–Staver's (1951) theory (referred to as theory B) which interprets sound waves in metals as collective plasma waves of randomly distributed positive ions whose interactions are screened by a free-electron gas.

According to theory A the isothermal bulk modulus is given by

$$K_T = \frac{kT}{\Omega}\left[\frac{(1+2\eta)^2}{(1-\eta)^4} + \frac{2ZE_F}{3kT} - A\left(\frac{V_m}{V}\right)^{1/3}\frac{T_m}{T}\right], \tag{8}$$

where

$$A = 10 + \frac{2ZE_F(T_m)}{5kT_m} . \tag{9}$$

Here Ω is the atomic volume, Z is valency, E_F is Fermi energy, and V_m is volume at the melting point. The hard-sphere packing fraction η is assumed to have the same value 0·45 for all liquid metals at the zero-pressure melting temperature. At other temperatures and pressures one has

$$\eta = \eta_V(T)\frac{V_m}{V} . \tag{10}$$

The constant volume value $\eta_V(T)$ has been calculated as a function of T by Ascarelli (1968) by solving a cubic equation which he fitted to the experimental data for the variation of pressure with temperature at constant volume for liquid sodium. From

K_T the velocity of sound is readily obtained by means of the thermodynamic relation

$$K_S = K_T \frac{C_P}{C_V} \tag{11}$$

and equation (3).

Theory B gives the sound velocity as

$$v = \left[\frac{N_i Z^2}{Mn(E_F)}\right]^{1/2}, \tag{12}$$

where N_i is ionic density, M atomic mass, and $n(E_F)$ electron density of states at the Fermi level. For free electrons this reduces to

$$v = \left(\frac{2ZE_F}{3M}\right)^{1/2}. \tag{13}$$

Webber and Stephens (1968) have found significantly better agreement with experiments if equation (13) is empirically modified to

$$v = \left(\frac{2E_F}{3M}\right)^{1/2}. \tag{14}$$

The physical reason for removing the $Z^{1/2}$ factor is not clear; nonetheless we shall employ the form (14) in our comparison. It follows from equations (13) or (14) that at varying temperatures and pressures v has only a volume dependence

$$v(V) = v(V_m)\left(\frac{V_m}{V}\right)^{1/3}. \tag{15}$$

In the case of mercury, Mott (1966) has suggested that $n(E_F)$ may differ from the value for free electrons. According to equation (12), this implies that equation (15) should become

$$v(V) = v(V_m)\left(\frac{V_m}{V}\right)^{1/3}\left(\frac{g}{g_m}\right)^{-1/2}, \tag{16}$$

where

$$g = \frac{n(E_F)}{n_f(E_F)}.$$

We refer to equation (16) as theory B′.

The theoretical expressions were evaluated with the use of experimental data for density and C_P/C_V. Other fixed-point parameters used are listed in table 3. For the 'pseudogap parameter' g for mercury we have linearly interpolated or extrapolated

Table 3. Parameters used for the evaluation of the theoretical velocity of sound in bismuth and mercury.

	Bismuth	Mercury
T_m (K)	544	235
ρ_m (kg m^{-3})	$1{\cdot}0057 \times 10^4$	$1{\cdot}3689 \times 10^4$
Ω (10^{-29} m^3)	$3{\cdot}46$ [a]	$2{\cdot}48$ [b]
ρ (kg m^{-3})	$1{\cdot}0022 \times 10^4$ [a]	$1{\cdot}3534 \times 10^4$ [b]
Z	5	2
$\frac{2ZE_F(T_m)}{15kT_m}$	146 [c]	103 [c]

[a] At $T = 573$ K, $P = 0$; [b] at $T = 298$ K, $P = 0$; [c] after Ascarelli (1968).

between the theoretical value $g = 0{\cdot}95$ at a density of $1{\cdot}3534 \times 10^4$ kg m^{-3} calculated by Chan and Ballentine (1972) and Mott's (1972) empirical estimate from thermoelectric power data of $g = 0{\cdot}7$ at a density of $1{\cdot}1 \times 10^4$ kg m^{-3}.

As is apparent from figure 4, the overall agreement between theory and experiment is quite poor. The discrepancies are much more serious for mercury than for bismuth. For mercury theory A predicts a value ~25% too small for v at 300 K and atmospheric pressure. In contrast to the experimental trend, v increases with T along isobars, and $(\partial v/\partial P)_T$ is about one-fifth of the measured value and decreases with T. Theory B gives a value for v at 300 K and atmospheric pressure in good agreement with the experiment; the correct trend for the temperature and pressure dependence of both v and $(\partial v/\partial P)_T$ is obtained; but the magnitudes of $(\partial v/\partial T)_P$ and $(\partial v/\partial P)_T$ are only one-fifth and one-tenth, respectively, of those observed. An attempt to correct for the deepening of the pseudogap with increased volume (theory B′) makes things even worse. Both the temperature and pressure dependence now emerge with the wrong sign!

In the case of bismuth, theory A overestimates the sound velocity by some 20% (note different scales on figure 4b) but gives the right trend for the temperature and pressure dependence in general. The observed pressure derivative $(\partial v/\partial P)_T$ is closely predicted, but the average $(\partial v/\partial T)_P$ is underestimated by a factor of five. It is interesting that at all pressures from 0 to 1 GPa (10 kbar) the theoretical velocity isobar has a maximum around 800 K. This is reminiscent of the abrupt change in $(\partial v/\partial T)_P$ at 853 K reported by Gitis and Mikhailov (1965) and attributed to structural rearrangement. Since theory A has no built-in feature to account for structural changes, the velocity maximum must have arisen from the experimental data for ρ and C_P/C_V used in the calculation. Our velocity data do not show a sharp change, but rather a distinct change of slope spread over 100 K or so, possibly because our data points were taken at steps of 100 K in the temperature range concerned. It is also likely that the actual change of slope is more gradual, as Webber and Stephens (1968) have mentioned. Examination of our data reveals that this change of slope is also present in the C_P isobars, but in the opposite direction. This might conspire with the shallow slope in the theoretical curve to magnify the slope change into a spurious peak. Theory B produced a velocity less than 10% higher than that observed at 550 K and zero pressure. Both $(\partial v/\partial T)_P$ and $(\partial v/\partial P)_T$ have the right sign. The magnitude of the temperature derivative is in much better agreement with experiment for bismuth than for mercury, although it is still underestimated by a factor of two. Discrepancy in $(\partial v/\partial P)_T$, however, is equally severe for both metals.

The experimentally determined variation of the Grüneisen parameter γ with T, P, and V are shown in figure 6. Theoretical predictions (not illustrated) based on theoretical values of v and observed values of α and C_P bear little resemblance to these experimental results. For both metals both theories (A and B) give values of γ increasing with V at constant T, and decreasing with T at constant V. In fact, the theoretical isotherms are almost perpendicular to the observed ones in all cases. Theoretical isobars are generally in better accord with experiments. Again the agreement is better for bismuth for which both theories have yielded fairly flat isobars. For mercury, γ increases with volume along all the isobars obtained from theory A, and along those isobars obtained from theory B isobars which are for pressures lower than 0·6 GPa (6 kbar). As for the magnitude of γ, theory B gives values differing by less than 20% from the observed results throughout the T, P domain of our experiments, whereas the values predicted by theory A are about 50% too large for bismuth and too small for mercury. Neither theory predicts any of the observed high-temperature or high-compression trends shown in figure 6.

Two plausible reasons can be cited to explain the drastic discrepancies between theory and experiment: (i) the theories used are oversimplified, and (ii) both molten mercury and bismuth are abnormal in certain respects. We shall elaborate this in the following paragraphs.

In theory A, in addition to using a hard-sphere model, Ascarelli (1968) neglected the atom-position-dependent part of the total binding energy of the system, considered the ions as point charges, and assumed the temperature variation of the hard-sphere radius—and hence the packing fraction η—to be the same for all metals, so that values derived from liquid sodium data can be applied to other metals. Actually Ascarelli (1968) himself has remarked on discrepancies found for the semimetals bismuth and antimony. We found here that it fares even worse in the case of mercury, especially in the variations with temperature and pressure.

In theory B, Bohm and Staver (1951) assumed the positive ions in the metal to be randomly distributed and approximated the interionic potential by a screened Coulomb potential between point charges. It is now evident from the experience in calculating the electrical (see Ziman, 1967, for a review) and electronic properties (Chan, 1971; Ballentine, 1975) of molten metals that erroneous results can be obtained through using inaccurate ionic distribution and unrealistic potentials. Without the Webber–Stephens empirical modification, the Bohm–Staver theory can give sound velocities up to several times larger than experimental values for polyvalent metals. Recently Tokita *et al.* (1973) have advanced a significant improvement to the Bohm–Staver theory by taking into account the positional correlation of positive ions through the introduction of the pair distribution function and by using interionic potentials based on Hasegawa and Watabe's (1972) theory of compressibility. Unfortunately, few data on the temperature and pressure variations of pair distribution functions are available, and great difficulties are encountered in deriving ion–ion potentials from the electron–ion pseudopotential, except for the alkali metals. For alkali metals, hard-sphere theory may be expected to provide satisfactory representation of the pair distribution function.

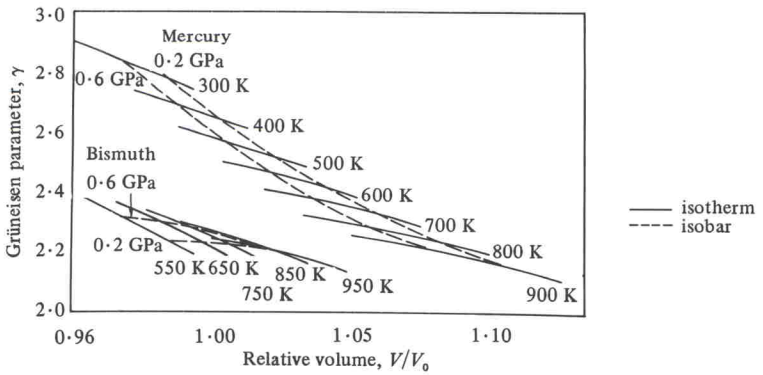


Figure 6. Grüneisen parameter for liquid mercury and bismuth in P–V–T space. V_0 represents volume under initial P, T conditions of present measurements.

4.4 *The anomalies of mercury and bismuth*

Having discussed the difficulties underlying the theory, we now proceed to consider the anomalous properties of molten mercury and bismuth. By virtue of its very low melting point, mercury is more amenable to experiment than any other liquid metal. It is therefore hardly surprising that a great wealth of data has been amassed for various physical properties of mercury. Some workers are tempted to extrapolate such data to the behavior of other molten metals under temperature and pressure

conditions at present unattainable in the laboratory. This is a precarious undertaking, for the very low melting point itself suggests that mercury is abnormal. Indeed the electronic transport properties of mercury and its alloys have been found to be radically different from those of other metals. For instance, both its electrical resistivity and Seebeck coefficient are two to three times larger than for cadmium and zinc, and the resistivity drops rapidly under pressure. Upon alloying, the anomaly usually disappears. Mott (1966) was able to explain most of these unusual properties by postulating for mercury a pseudogap, that is a depleted electron density of states near the Fermi level; E_F. However, Evans (1970) was able to explain the electrical resistivity without invoking the pseudogap, by taking into account the effects of the proximity of the d band to the conduction band in constructing a pseudopotential for mercury. Using this same pseudopotential, Chan and Ballentine (1972) have calculated the density of states and found the pseudogap to be far shallower than Mott had assumed; furthermore, the trough of the gap lies below E_F. We have seen (theory B′, figure 4a) that assuming the pseudogap to depend solely on density and to deepen to the value required by Mott (1972) at a density of $1{\cdot}1 \times 10^4$ kg m^{-3} makes theory B worse and leads to temperature and pressure variations for v qualitatively opposite to observations. This may be interpreted to mean that there is hardly any pseudogap at the densities concerned. Alternatively, we can say that as the temperature is raised, the energy bands are broadened, overlapping more and more and eventually filling up the pseudogap.

It is not possible at present to estimate this effect quantitatively, but if we assume that the pseudogap parameter is 0·8 under room conditions, that the temperature effect dominates for densities in our experimental range, and that the pseudogap is completely filled up at 1200 K where we expect γ to become temperature independent, then $(\partial v/\partial T)_P$ predicted by theory B would be modified in such a way that the observed result is closely approximated and the temperature dependence of γ would be less different from experimental. We can also partially explain the large volume dependence of v at constant T (two to three times larger than in other polyvalent metals) using the fact that, in the absence of thermal band broadening, the density effect becomes more prominent. It should be mentioned that, even if this turns out to be true, it does not necessarily imply that the calculation of Chan and Ballentine (1972) is incorrect. Because the results of that calculation are sensitive to the pseudopotential employed, the possibility exists that a pseudogap might be predicted if a different pseudopotential, such as the one proposed by Devillers *et al.* (1973), were used.

For densities of $8{\cdot}5 \times 10^3$ kg m^{-3} and below, the work of Hensel and Franck (1966) and other authors cited by Mott (1972) seems to provide good evidence for the existence of the pseudogap. On the other hand, data for higher densities ($1{\cdot}1 \times 10^4$ kg m^{-3} and over) do not lend themselves to unambiguous interpretation.

Thus this pseudogap question remains open. It is, of course, also possible that the unusual behavior of the sound velocity and other equation-of-state parameters for mercury can, like that of the electrical properties, be explained by the peculiar nature of the pseudopotential.

Bismuth differs from mercury, and for that matter from most other metals, in being a semimetal with very loose packing and hompolar bonding in the solid state. On melting, the packing becomes much closer, as reflected in its decrease in volume and also in its large entropy change. Bismuth differs less from a normal metal in the liquid state than it does in the solid state. Nevertheless, the structural change on melting is incomplete and further changes occur in the liquid range. Such structural rearrangement has been observed directly by diffraction experiments (Dutchak, 1961), as well as indirectly by measurements of sound velocity (Gitis and Mikhailov, 1965)

and electrical resistivity (Goryaga, 1956). The large increase of $(\partial v/\partial T)_P$ with rising T observed in the present investigation (table 1) is an example of the effect of structural changes. On the other hand, the tendency of the Grüneisen parameter to become independent of temperature (figure 6) at high compression, observed also for water (Knopoff and Shapiro, 1970) but not for mercury, may be related to contraction on melting. For bismuth and water isothermal compression removes the liquid further away from the freezing point, whereas for mercury this brings the liquid closer to freezing. If this proves to be the case, then temperature independence of γ at high compression may not be a general property of liquids.

5 Conclusions

It is apparent from the discussion in the preceding section that much of the observed behavior of the sound velocity and equation-of-state parameters at high temperatures and pressures may be due to the abnormal nature of molten mercury and bismuth. Therefore it would be unwise to attempt any sweeping generalization concerning these properties for other molten metals. There is one trend, however, which we feel may represent normal liquid metal behavior, namely the tendency of the Grüneisen parameter to become independent of temperature and pressure at large volume. In view of the foregoing discussions, we expect mercury and bismuth to become more or less normal at high temperatures, mercury upon filling up of the pseudogap in the electron density of states, and bismuth upon completion of structural changes. It would be most interesting to verify or disprove this hypothesis by experiments similar to those reported here on simple liquid metals such as the alkali metals and some normal polyvalent metals like aluminum. On both theoretical and experimental grounds a comparison of observed data for alkali metals with the theories of Hasegawa and Watabe (1972) for compressibility, and Tokita *et al.* (1973) for sound velocity, would be a desirable step toward further understanding of the equation of state for liquid metals.

Acknowledgements. The two lead authors (H. S. and M. M.) would like to thank J. Brierly and L. Hill for their administrative support and encouragement during the experiments. G. Kirchner and O. Wallen contributed through their ingenuity in the laboratory. The bulk of this work was supported by the A.E.C. Constructive criticism by an anonymous reviewer was greatly appreciated. The editors deserve special thanks for their efforts to ensure the correctness of all unit conversions.

References

Ascarelli, P., 1968, *Phys. Rev.*, **173**, 271-274.
Ballentine, L. E., 1975, in *Adv. Chem. Phys.*, **31**, 263-327.
Bohm, D., Staver, T., 1951, *Phys. Rev.*, **84**, 836-837.
Bridgman, P. W., 1949, *The Physics of High Pressure* (Bell and Sons, London), p.130.
Chan, T., 1971, Ph. D. Thesis, Simon Fraser University, Burnaby, B. C., Canada.
Chan, T., Ballentine, L. E., 1972, *Can. J. Phys.*, **50**, 813-820.
Davis, L. A., Gordon, R. B., 1967, *J. Chem. Phys.*, **46**, 2650-2660.
Devillers, M. A. C., Young, W. H., de Vroomen, A. R., 1973, *J. Phys. F.*, **3**, L220-L224.
Dutchak, Ya. I., 1961, *Fiz. Met. Metalloved.*, **11**, 290-295.
Evans, R., 1970, *J. Phys. C: Met. Phys. Suppl.*, **3** (2), S137-S152.
Even, U., Jortner, J., 1974, *Philos. Mag.*, **30**, 325-334.
Featherston, F. H., Neighbours, J. R., 1963, *Phys. Rev.*, **130**, 1324-1333.
Flinn, J. M., Jarzynski, J., Litovitz, T. A., 1971, *J. Chem. Phys.*, **54**, 4331-4340.
Gitis, M. B., Mikhailov, I. G., 1965, *Akust. Zh.*, English translation in *Sov. Phys.-Acoust.*, **11**, 372-375 (1966).
Goryaga, G. I., 1956, *Vestn. Mosk. Univ.*, **1**, 79-85.
Grindley, T., Lind, J. E., Jr., 1971, *J. Chem. Phys.*, **54**, 3983-3989.
Hasegawa, M., Watabe, M., 1972, *J. Phys. Soc. Jpn.*, **32**, 14-28.
Hensel, F., Franck, E. U., 1966, *Ber. Bunsenges Phys. Chem.*, **70**, 1154-1161.
Ivanov, B. M., 1969, *Teplofiz. Vys. Temp.*, English translation in *High Temp. (USSR)*, **7**, 834-840 (1969).

Jarzynski, J., 1963, *Proc. Phys. Soc. (London)*, **81**, 745-750.
Kelley, K. K., 1949, U.S. Bur. Mines, Bull.No.476, *Critical Evaluation of High-Temperature Heat Capacities of Inorganic Compounds.*
Kikoin, I. K., Senchankov, A. P., 1967, *Phys. Met. Metallogr. (USSR)*, **24** (5), 74-89.
Knopoff, L., Shapiro, J. N., 1970, *Phys. Rev.* B, **1**, 3893-3895.
Margrave, J. L., 1970, *High Temp. - High Pressures*, **2**, 583-586.
McSkimin, H. J., 1961, *J. Acoust. Soc. Am.*, **33**, 12-16.
Mott, N. F., 1966, *Philos. Mag.*, **13**, 989-1014.
Mott, N. F., 1972, *Philos. Mag.*, **26**, 505-522.
Postill, D. R., Ross, R. G., Cusack, N. E., 1968, *Philos. Mag.*, **18**, 519-530.
Seemann, H. J., Klein, F. K., 1965, *Z. Angew. Phys.*, **19**, 368-374.
Spetzler, H., 1970, *J. Geophys. Res.*, **75**, 2073-2087.
Spetzler, H., Sammis, C. G., O'Connell, R. J., 1972, *J. Phys. Chem. Solids*, **33**, 1727-1750.
Spetzler, H., Meyer, M., Boucher, G., 1974, *High Temp. - High Pressures*, **6**, 529-532.
Tokita, M., Yokota, I., Katayama, S., 1973, *Solid State Commun.*, **13**, 1087-1089.
Webber, G. M. B., Stephens, R. W. B., 1968, *Physical Acoustics*, volume 4B, Ed. W. P. Mason (Academic Press, New York), pp.53-97.
Ziman, J. M., 1967, *Adv. Phys.*, **16**, 551-580.

© 1975 a Pion publication printed in Great Britain